CORE
Metadata, citation and similar papers at core.ac.uk
Provided by Elsevier - Publisher Connector

Polymer 52 (2011) 2979–2990

Contents lists available at ScienceDirect

Polymer

journal homepage: www.elsevier.com/locate/polymer

Feature Article

Failure mechanisms in polyolefines: The role of crazing, shear yielding and the entanglement network

Rudy A.C. Deblieck [b,*], D.J.M. van Beek [a], Klaas Remerie [a], Ian M. Ward [c]

[a] SABIC, Technology & Innovation STC Geleen, PO Box 319, 6160 AH Geleen, The Netherlands
[b] DSM Resolve, PO Box 18, 6160 MD Geleen, The Netherlands
[c] School of Physics and Astronomy, University of Leeds, LS2 9JT Leeds, UK

ARTICLE INFO

Article history:
Received 22 October 2010
Received in revised form
16 February 2011
Accepted 29 March 2011
Available online 22 April 2011

Keywords:
Polymer science & technology
Polyethylene
Polypropylene

ABSTRACT

Macroscopic deformation and failure modes of polyolefines are reviewed in terms of deformation and failure models based on the craze initiation and propagation model of Kramer–Berger and the craze–crack transition model of Kramer–Brown. Although these models were formulated for amorphous polymers they are also valid for semi-crystalline polymers. The important role of the underlying molecular entanglement network in this approach is reflected by the strain hardening behaviour which is shown to be a robust measure for predicting slow crack growth performance. The polymer network response explains the experimentally observed presence of two Brittle–Ductile transitions, one at low temperature or high strain rates, linked with chain scission which dominates crazing, the other at elevated temperatures or low strain rates which involves disentanglement crazing. The relation between these two Brittle–Ductile transitions and the major transition temperatures for molecular mobility such as the glass transition and the crystal α relaxation temperature are discussed. Valid strategies for increasing the crack propagation resistance in polyolefines are reviewed. Finally an outlook for further research to complement the present knowledge base is formulated.

© 2011 Elsevier Ltd. Open access under CC BY-NC-ND license.

1. Introduction

Failure modes generally known as slow crack growth (SCG) and rapid crack propagation (RCP) turn out to be the major phenomena responsible for life span reduction in most applications. It is therefore important to understand the mechanisms underlying crack growth and be able to evaluate, rank and finally tailor the resistance of materials against it.

In the present article the phenomenon of SCG will be physically analysed by existing deformation models of craze propagation and craze–crack transition, whereby the importance of the molecular network is highlighted. Understanding structure–property relationships in polymers is a critical step towards tailoring the required mechanical properties of the end product. These insights can be used to design new test methods based on intrinsic material properties that allow prediction and/or ranking of materials for their SCG performance.

Polyolefines tend to be found in applications where a long service life time is required, such as automotive or pipe applications. Several developments have brought important improvements in this respect, such as the development of high impact resistant Polypropylene copolymers and bimodal High Density Polyethylene pipe grades.

2. Crazing and shearing

Brittle failure of polymers basically involves the propagation of a crack through the material. Although toughness may be defined in a number of different ways, most of them involve the amount of energy absorbed in a mechanical test. Fracture Mechanics defines toughness operationally as the resistance to crack propagation as measured in a dedicated test [13]. In polymers the resistance to this crack propagation is governed by local plasticity which is reflected in the micro-deformation mechanisms.

A polymer fails either through deformation without change of volume (i.e. no creation of internal surface) denoted as ***shear***, or deformation accompanied by volume increase denoted as ***crazing*** [28].

Shear within this context is identical with flow of the continuum. In rheological terms this flow involves elongational or shear deformation. This continuum flow occurs at the macroscopic yield point that is associated with the engineering yield stress. The

* Corresponding author. Tel.: +31 (0) 46 476 1661; fax: +31 10 264 4780.
E-mail address: rudy.deblieck@dsm.com (R.A.C. Deblieck).

0032-3861 © 2011 Elsevier Ltd. Open access under CC BY-NC-ND license.
doi:10.1016/j.polymer.2011.03.055

phenomenon of shearing may occur in macroscopic tensile tests as localised shear bands, or homogeneous shear flow.

3. Crazing

3.1. Crazing phenomenology

Crazes as a phenomenon are first created, then they propagate and terminate turning into a crack. Crazing was first described morphologically by Kambour in 1973 [15]. The structural appearance of crazes is best observed by means of TEM on thin films, a method developed by Donald et al. [17,18,42] An example is shown for polystyrene [19] in Fig. 1.

From Fig. 1 it is clear that a craze consists of a network of cross-tied fibrils crossing the craze planes from which the network grows by pulling out fresh material from a so-called stress activated active zone as it shown schematically in Fig. 5. These craze planes are always perpendicular to the main stretch direction.

Crazes are **initiated** when the external stretch causes a microscopic void to open up at a stress concentration created by a pre-created notch, a heterogeneity in the molecular network or a foreign particle. It is clear that the probability of such microscopic voids to occur is dependent on the local stress situation. Kramer proposes that in the craze nucleation mechanism [20], plane strain is more likely to open up such voids, than plane stress. More recently, Van Melick et al. [21] elegantly demonstrated this concept by means of micro indentation and constitutive modelling to establish a critical hydrostatic stress criterion for craze initiation in glassy polymers. They found that the critical hydrostatic stress is typically in the order of the van der Waals surface energy ($\sim$40 mJ/m^2) and that it increases with increasing network density.

This microscopic void will **propagate** in a plane perpendicular to the highest principal stress and will be stabilised temporarily by fibrils spanning the craze. Eventually, the stabilisation by fibrils will fail and a craze–crack transition occurs and actual failure sets in [20,25]. The macroscopic stress required for the craze to propagate is the so-called craze stress. This mechanism is schematically represented in Fig. 2.

Crazing was initially a phenomenon that was reported solely for glassy, amorphous polymers but it also occurs in semi-crystalline polymers as reported by Plummer et al. [1,23] and Thomas et al. [3]. It is observed that the typical fibril sizes tend to be an order of magnitude coarser in the case of semi-crystalline polymers (200 nm) compared to amorphous polymers (20 nm).

3.2. Mechanisms of craze propagation and craze stress

Craze propagation [19,20,24] and the craze–crack transition [25,27] have been extensively studied in amorphous polymers

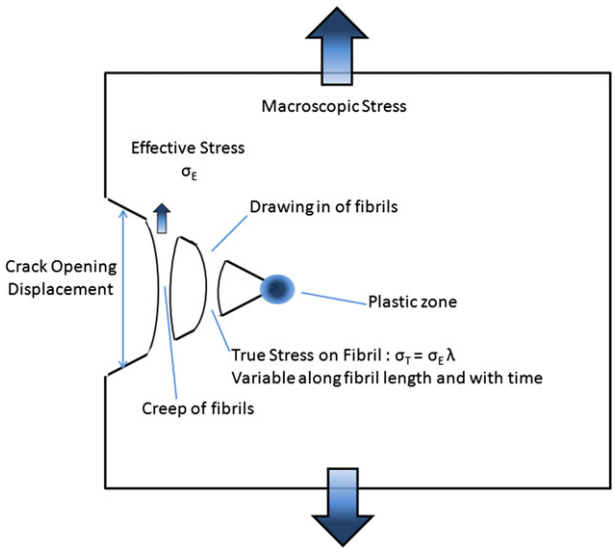

Fig. 2. Craze–crack and craze propagation represented schematically. The propagation goes from left to right. The principal stress acts in the up-down direction. (remade after O' Connell et al. (1995) [6] with kind permission of Elsevier Limited).

below the glass temperature (T_g) by Kramer and his collaborators. We will review the rationale behind the approach followed by Kramer to demonstrate that the continuum model and the physico-chemical specifications used to describe craze propagation in amorphous glassy polymers are not limited to amorphous polymers.

Kramer [20] starts from the idea that the propensity to create new surface will favour the prevalence of crazing, as originally proposed by Argon [26]. The energy needed to create new surface, Γ, will therefore be the determining factor and is considered to consist of two contributions as shown in Equation (1):

$$\Gamma(\gamma, \nu_e) = \gamma + \frac{1}{4}\nu_e U d \tag{1}$$

where the surface energy, γ, is the van der Waals cohesive energy between molecules. ν_e is the effective entanglement density i.e. the entanglements that are able to convey load at the time scale of the observation, d is the end-to-end distance between effective entanglements and U is the energy needed to fracture a covalent chain. Therefore, the second term describes the contribution of covalent bonds crossing the created surface which are able to contribute to the cohesion by bearing load.

In this definition, a chemical cross link is counted as an effective entanglement. The factor ¼ takes into account the two surfaces

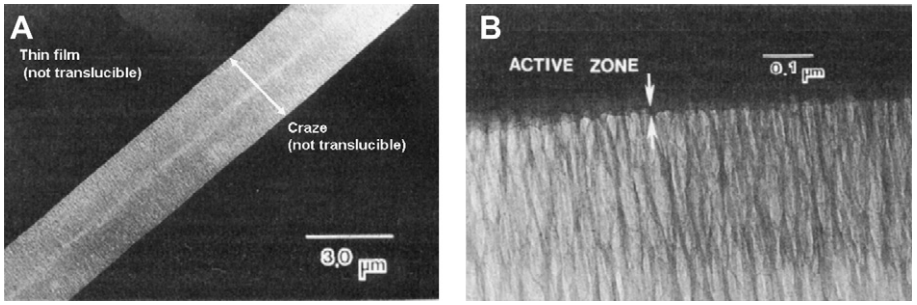

Fig. 1. Crazing as observed by Transmission Electron Microscopy in a thin film of polystyrene. The white arrow (in 1A) shows the craze opening and indicates the direction of the external load. In 1B a close up is shown of the craze micro-morphology consisting of the fibrillar network as it is being pulled from the stress activated craze boundary. (adapted from Berger et al. (1987) [19] with kind permission of American Chemical Society).

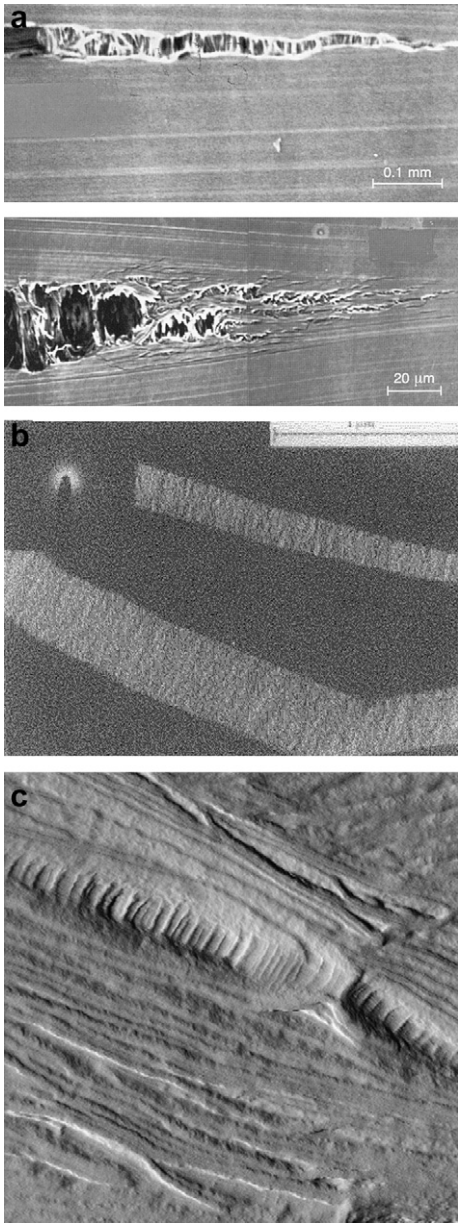

Fig. 3. a) Craze fibrillar network and the craze–crack transition in PE (upper) in addition, multiple crazing around the craze tip is revealed (lower). (reproduced from "Crack Growth in PE" PhD thesis of T. Riemslag (1997) University of Delft [2] with kind permission of the author). b) Crazing as observed by Transmission Electron Microscopy in a thin film of spherulitic isotactic polystyrene at room temperature. (reproduced from Plummer et al. (1994) [23] with kind permission of John Wiley and Sons). c) Crazing and coalescence of crazes as observed by tapping mode Atomic Force Microscopy,. The width of the image is 1.5 μm (reproduced from Thomas et al. (2007) [3] with kind permission of Elsevier).

created in the free surface and the fact that one effective entanglement actually involves two molecular stems for load transfer. $\nu_e d$ scales as $\nu_e^{1/2}$ except for very short chains [20], which implies a strong dependence of Γ on ν_e. Actual values are about 40 mJ/m^2 for the first term (γ). For a polymer with an entanglement density of $3\cdot10^{25}$/m^3 (i.e. Polystyrene) the second term has about the same magnitude as the first term, hence $\Gamma \approx 80$ mJ/m^2 [20,24,78].

The effective entanglement density as defined above is not necessarily identical to the rheological definition of the entanglement density in terms of the melt elasticity response at the rubber plateau, although it will be of the same order of magnitude.

The craze stress can be derived from an optimisation of the growth rate of a craze with respect to the craze microstructure (i.e. fibril diameter). Following Argon [22] and Kramer et al. [16,20,24] the tip of a craze is considered to be a load activated melt that transforms into fibrils driven by surface energy, via a Taylor meniscus instability as shown schematically in Fig. 4. The validity of the principle of craze propagation via a Taylor meniscus instability for semi-crystalline polymers is convincingly supported by the work of Thomas et al. [3].

Starting from a power-law like behaviour of the material, which is drawn into the craze fibrils from the active zone as shown in Figs. 1 and 5, the craze stress σ_{cr} is found to be proportional to the square root of the surface energy [24], as described by Equation (2).

$$\sigma_{cr} \propto \sqrt{\sigma_y \Gamma(\gamma, \nu_e)} \tag{2}$$

The strain rate dependence of the craze stress is relatively weak and mainly determined by the strain rate dependence of the yield stress σ_y and to a lesser extent by the increase of the number of effective entanglements with strain rate.

The craze microstructure (i.e. the fibril diameter D) is directly related to the surface energy Γ [20,24]

$$D \propto \frac{\Gamma}{\sigma_{cr}} \tag{3}$$

3.3. Craze–Crack transition

Once a craze is formed and propagates it will eventually fail via a so-called craze–crack mechanism. The Brown–Kramer craze–crack transition model elegantly describes this transition [25,27] based on a fracture mechanics approach, calculating the critical stress intensity or the strain energy release rate of the mechanically anisotropic fibrillar network within the craze. In this calculation the stress transfer by the orthotropic network of cross tie fibrils is an essential contribution to generate a stress concentration at the craze–crack interface fibril. This approach allows formulating a stress (force) criterion for the failure of the fibril at the craze–crack transition as schematically shown in Fig. 6. This is equally valid for glassy amorphous and semi crystalline polymers as Fig. 3 demonstrates. The strain energy release rate for crack opening, G_{1c}, as a proportionality as shown in Equation (4).

$$G_{1c} \propto (\Sigma_e f_s)^2 \tag{4}$$

In which Σ_e is the network density expressed as the number of effectively load bearing chains per unit volume and f_s is the force needed to break one molecular chain.

To demonstrate the physical feasibility of this approach, Brown [25] obtains a value for the force required to break a carbon–carbon bond in a single molecular chain (f_s) of $1.4\cdot10^{-9}$ N when using the G_{1c} value obtained for polymethylmethacrylate (PMMA) and by using $\Sigma_e = 2.8\cdot10^{17}$ m^{-2}. The value of f_s is within the range of

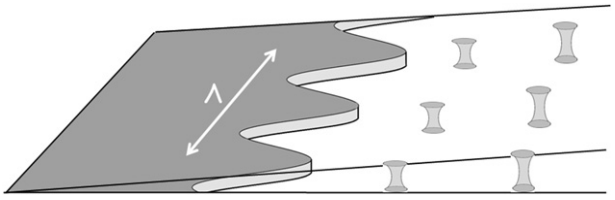

Fig. 4. Stress induced melt at a craze tip transforms into fibrils via a surface tension driven Taylor meniscus instability. (remade after Kramer (1983) [20] with kind permission of Springer Science & Business Media).

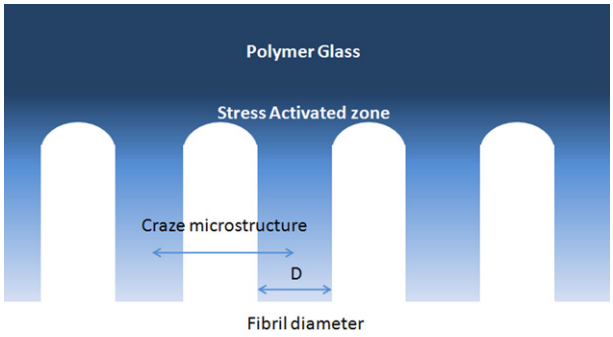

Fig. 5. The drawing of fibrils in a craze from the stress activated zone in the polymer glass. The fibril diameter and its periodicity, the so-called craze microstructure, depend on the surface tension of the polymer. (remade after Kramer et al. (1990) [24] with kind permission of Springer Science & Business Media).

$3 \cdot 10^{-9}$ N estimated by Kausch [28] for the chain breaking force and between $2.5–12 \cdot 16^{-9}$ N estimated for f_s by Odell and Keller [29] from elongational flow experiments on polyethylene (PE).

Equation (4) implies that, since the fracture force of a covalent backbone bond has a fixed order of magnitude for all polymers irrespective of whether they are glassy amorphous or semi-crystalline, the greater the number of effectively entangled (or cross linked) chains which cross the fracture interface of the fibril, the tougher the polymer will be. It is quite plausible to assume proportionality between the effective entanglement density and Σ_e.

It can be concluded that both the craze propagation criterion and the craze–crack transition stress criterion rely primarily on the effective entanglement density, a molecular concept that is not compromised by whether a polymer is semi-crystalline or not.

4. Shearing-yield stress

Shearing is a plastic deformation mechanism characterised by a continuum flow, without the creation of an internal surface. From the viewpoint of energy dissipation and toughness considerations, shearing is far more effective than crazing because the entire volume of the plastically deforming material is participating in the energy dissipation. Formally, shearing occurs when the formation of internal surface is prevented and it will therefore be the aim to prevent this creation of internal surface by maximising Γ and facilitating the ease of flow by lowering the resistance to macroscopic flow, i.e. the yield stress.

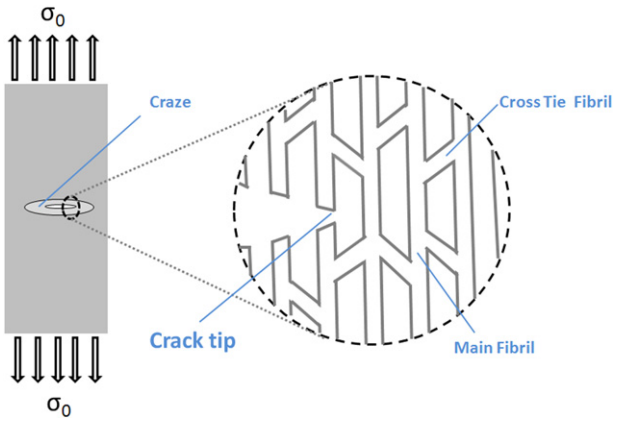

Fig. 6. Craze–crack tip model used by Hui et al. (remade from Hui et al. (1992) [27] with kind permission of American Chemical Society).

Empirically it is known that the yield stress of amorphous polymers below T_g is proportional to the Cohesive Energy Density δ^2 (where δ represents the solubility parameter) and the difference between T_g and temperature T as shown in Equation (5) [30].

$$\sigma_y = \delta^2 (T_g - T) G(C_\infty) \tag{5}$$

where G represents the intra chain contribution to yield stress which depends essentially on the characteristic ratio C_∞. The characteristic ratio is defined as the ratio of the mean-square end-to-end distance, of a real linear polymer chain in a theta state to the same distance in an ideal 'pearls and beads' chain with the same step length and number of steps [31]. The strain rate dependence of the yield stress is conveniently described by an Eyring thermally activated flow process as described in Equation (6) [14].

$$\dot{\varepsilon} = \dot{\varepsilon}_0 e^{-\left(\frac{\Delta H}{RT}\right)} \sin h\left(\frac{v\sigma_y}{RT}\right) \tag{6}$$

where ΔH is the activation enthalpy, v is the activation volume for shear flow under a shear stress σ_y.

For semi-crystalline polymers Equation (5) cannot be used because the yield stress in semi-crystalline polymers is not solely determined by the distance to T_g. In that case the Eyring Equation (6), which generally describes activated flow via the activation enthalpy ΔH, may be used to describe the yield stress and its temperature and rate dependence.

5. The competition between shearing and crazing

5.1. Shearing crazing transitions

Although the eventual failure mechanism following crazing or shearing will be either craze–crack failure or fracture of the plastically yielded zone after shear deformation, it is the preceding deformation mechanism that will determine the amount of energy dissipation. Crazing, even when it occurs as multiple crazing [32], is not a desired energy dissipation mechanism because the volume involved in the crazing mechanism is negligible due to the severe strain localisation within the craze.

It is clear that depending on whether the yield stress or the craze stress is lower, the prevailing micro-deformation mechanism will shift from crazing to shear deformation or vice versa. Therefore, shearing being the most effective energy dissipation mechanism, the craze stress needs to be higher than the yield stress. Following Equation (2) this can be achieved by increasing Γ independently from the yield stress. Equation (1) shows that this is done by increasing the number of effective entanglements or the number of crosslinks.

There are two possible mechanisms to create internal surface by crazing:

1) At low temperatures and high strain rates the characteristic time for disentangling a chain becomes long with respect to the time scale of the experiment and surface will be created as the chains will tend to break. In this limit both terms in Equation (1) contribute fully to the surface energy Γ.
2) At elevated temperatures and low strain rates chain relaxation becomes relatively faster compared to the time scale of the deformation process, and new surface will predominantly be formed by intermolecular separation and chain disentangling. In this case the surface energy is dominated by the van der Waals contribution γ in Equation (1).

Kramer and Berger have successfully described the chain disentangling process as a thermally activated process to describe the

onset of disentanglement crazing at high temperatures and/or low strain rates [24]. Thermal activation leads to a gradual transition from low craze stresses at high temperatures or low strain rates to high craze stresses at low temperatures and high strain rates.

The craze stress and the yield stress can be plotted as a function of temperature as shown for polycarbonate in Fig. 7.

Fig. 7 demonstrates that on decreasing the temperature a transition from disentanglement crazing to shearing occurs at about 28 °C below T_g. This transition is caused by the effect of the very high entanglement density of polycarbonate that increases the craze stress beyond the yield stress with decreasing temperature.

At lower temperatures (i.e. about 90 °C below T_g) a transition from shearing to scission crazing is to be expected. Due to the stronger increase of the yield stress with decreasing temperature, the craze and shear stress lines will cross again.

The dynamics of disentangling and the effect of rate and time on the process of disentanglement crazing in semi-crystalline polymers has been extensively reviewed by Kausch and Michler in 2005 [78].

5.2. Two shearing–crazing transitions and the shearing plateau

From the above framework based on Kramer's work it is clear that amorphous polymers potentially feature two shearing–crazing transitions. Since crazing is eventually associated with brittle failure and shearing with ductile failure these transitions may also be denoted as Brittle–Ductile (BD) transitions. One transition occurs at low temperatures/high strain rates and is governed by chain scission crazing followed by craze–crack failure. The other transition occurs at high temperatures/low strain rates and it is governed by disentangling chains. The existence of two shearing crazing transitions and an intermediate plateau where the dominant deformation mechanism is shearing was experimentally observed by Donald et al. [17,18,42] when studying the Strain on Deformation Onset (SDO) of thin polymer films. SDO is the nominal strain at which the first deformation phenomena appear in thin films as observed under a light microscope. Because of the larger strain localisation in crazing the nominal strain will be lower for crazing than for shearing deformation. The SDO as a function of temperature, or time is shown schematically in Fig. 8.

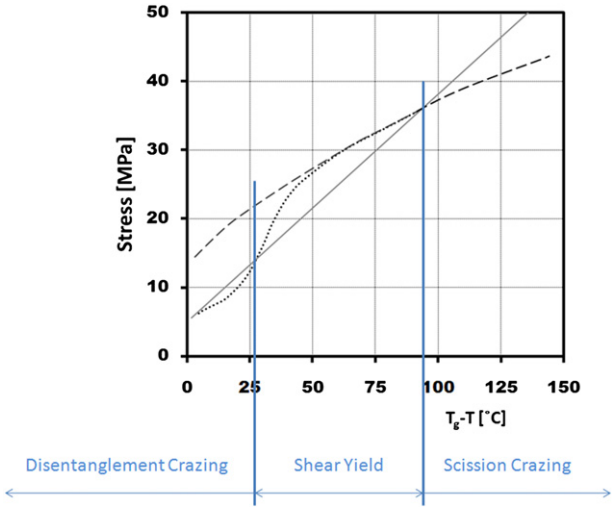

Fig. 7. Yield stress (solid line) and craze stress (the dotted line is the line taking into account the thermally activated disentanglement of molecular chians, whereas the striped line, denoted scission crazing is the calculated craze stress assuming that Equation (1) is valid) as a function of temperature for polycarbonate. (redrawn and extrapolated from Kramer et al. (1992) [24] with kind permission of Springer Science & Business Media).

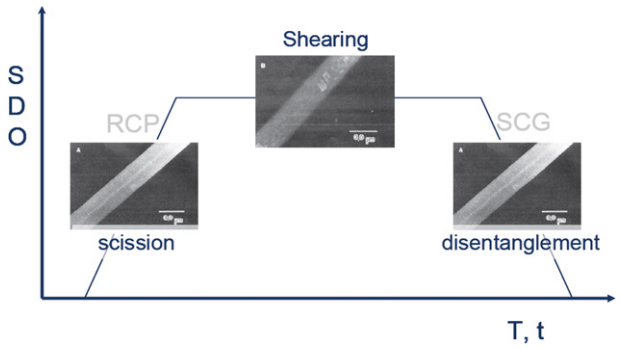

Fig. 8. Schematic representation of the Crazing - Shearing transitions in a Strain on Deformation Onset (SDO) setup.

Whether the occurrence of craze–crack failure at high strain rates (and or low temperatures) is limited to thin films or whether it occurs also for thicker objects is dependent on the multi-axiality of the local stress state. As the object becomes thicker, this stress state changes from plane stress to plane strain. Increasing multi-axiality of the local stress state is expected to favour the initiation and propagation of crazes and it will therefore shift the lower craze–shear transition to higher temperatures. However, the qualitative features of the process will not change with object size.

As stated before, the main difference between the lower and the higher BD transition lies in the different response of the molecules to the creation of internal surface at the given condition. At the lower BD transition the shearing deformation is prevented because the yield stress at low temperatures exceeds the craze stress. On the other hand, the absence of thermally activated reptation will prevent molecules from disentangling hence internal surface will solely be created by chain scission. At the higher BD transition (or low strain rates) it is precisely the ability of molecules to reptate that allows the easy creation of internal surface. Because disentanglement requires mobility of molecular chain segments between entanglements, the higher BD transition is be associated with T_g as demonstrated in Fig. 7.

For semi-crystalline polyolefines, featuring more mobile chain segments, T_g is usually much lower than for glassy amorphous polymers and it is to be expected that the BD transition will be determined by the collective mobility transition before melting such as the α-transition in polyethylene (PE). Indeed, it is observed that PE may feature a ductile, shearing response down to about −50 °C, which is still well above T_g. For polypropylene (PP) with a T_g of 0 °C, much closer to the typical application temperature, the influence of T_g will be more prominent. As a consequence, PP fails in a brittle mode below a temperature of ~60–70 °C, which is well above T_g. That this BD transition is considerably higher than T_g for both PE and PP, is a consequence of the plane strain load situation within the bulk of a test sample. It is by changing this stress condition to plane stress by the introduction of a disperse rubber phase that one is able to shift the BD transition to lower temperatures [34–41].

Since the upper BD transition is related to molecular disentangling phenomena or chain slip in crystals, increased resistance to disentangling or slip in crystals (i.e. a higher transition temperature or more tie molecules) will be found upon increasing the molecular mass. This phenomenon is directly related to the extension of the rubber plateau to higher temperatures, or lower frequencies in a dynamical mechanical experiment. This is equivalent to the increased maximum relaxation time upon increasing the molecular mass.

Longer molecular relaxation times will shift the disentanglement transition towards higher temperatures, times or lower strain

rates. Because of this inherent time dependency, this concept includes consideration of the speed of failure. At short time scales, or low temperatures, the scission crazing mechanism is essentially the mechanism for RCP, whereas at increased temperature, or long time intervals, the mechanism will be termed SCG as indicated in Fig. 8.

The same figure with stress on the ordinate is well known as the Davidenkov plot shown in Fig. 9 [14]. The typical Davidenkov plot refers only to the lower BD transition; a second 'DB' transition would be the intersection with a 'fracture' line associated with the pull out of entanglements at lower stress as indicated by the dotted 'disentanglement crazing' line as shown in Fig. 9.

The presence of such a disentanglement line is also proposed by Michler [33].

5.3. The BD transitions in semi-crystalline polymers

The general scheme of craze–shear competition is also valid for semi-crystalline polymers [1,3,23] where experimental observations of the failure mechanism for PE [5,6] support the concept of a shear plateau between two transitions. Two BD transitions (T_{BD} and T_{DB}) with a ductile plateau were observed in a series of fully notched tensile tests in several types of PE as a function of strain rate and temperature. A typical result is shown in Fig. 10.

O'Connell et al. [6] represented the experimental findings shown by Fig. 10 as a Davidenkov like plot as function of strain rate which is reproduced in Fig. 11. The strain rate dependency of the BD transitions is in agreement with the shearing-crazing concepts presented above. As in Fig. 9, it is assumed that the yield line is crossed by an extra chain disentanglement process which governs fracture at low strain rates.

6. A material intrinsic parameter describing the resistance to SCG

6.1. Effective entanglement density as a toughness measure

From the above considerations, it is clear that the resistance to SCG is proportional to the magnitude of the craze stress which is mainly determined by the effective entanglement density. So the intrinsic resistance of a material to SCG is best measured by assessing the effective entanglement density or the amount of load bearing chains per surface unit Σ_e. The total entanglement density

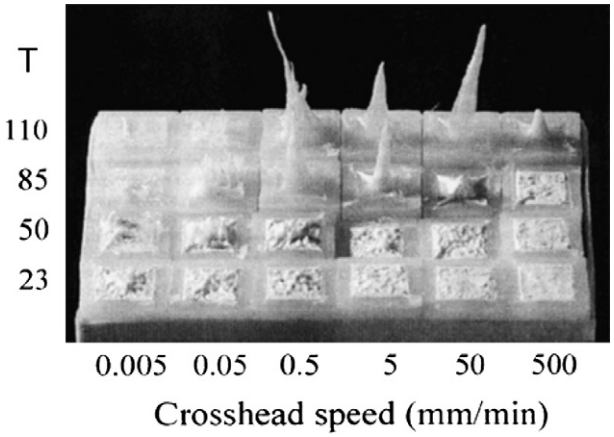

Fig. 10. Brittle–ductile transitions in natural drawn PE after O'Connell et al. (reproduced from O'Connell et al. (2002) [7] with kind permission of John Wiley and Sons).

for a pure polyolefine melt according to Richter et al. [46] scales as denoted by Equation (7).

$$\nu \propto C_\infty^{1.4} \left(\frac{\rho}{m_0}\right)^{2.2} l_0^{3.6} \tag{7}$$

where C_∞ is the characteristic ratio. Basically C_∞ is a measure of the segmental stiffness or the persistence length of the polymer. ρ is the density, m_0 the mass of a monomer and l_0 the contour length of this monomer. Equation (7) leads to the conclusion that slender molecular backbones favour high entanglement densities. To a lesser extent chain stiffness also contributes to the entanglement density via C_∞. The latter conclusion is actually counterintuitive because one would expect a flexible molecule to be more apt to entangle. Wu [43–45] offers an expression for the entanglement density which features proportionality with C_∞^{-2}. However, as the influence of the contour length density is neglected by Wu, this proportionality is incorrect. Furthermore, the behaviour of C_∞ and molecular weight between entanglements (M_e) with temperature follows a significantly different functionality, which clearly indicates that a simple proportionality of ν with C_∞^{-2} is erroneous [46].

For an entanglement to be truly effective (i.e. load bearing on the time scale of the experiment) it is required that $M_n \geq \zeta M_e$. For

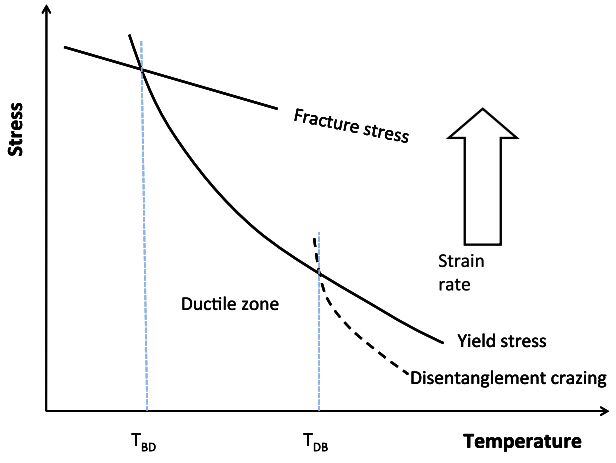

Fig. 9. Davidenkov plot of the BD transition. The brittle fracture failure line at high temperatures due to disentanglement crazing is added as a dotted line leading to a second DB temperature. The arrow indicates the general influence of increasing strain rate. (redrawn from Ward (1983) [14] with kind permission of John Wiley and Sons).

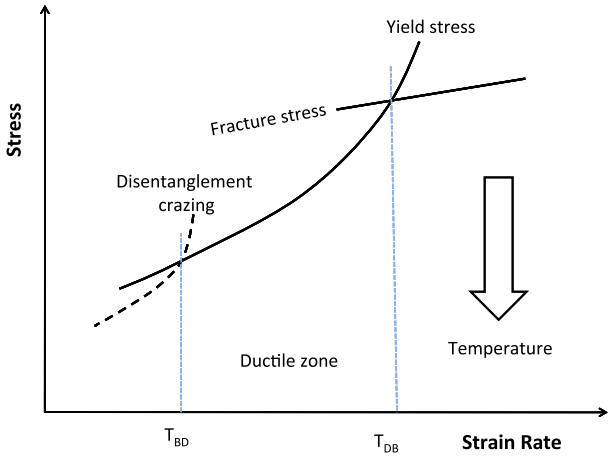

Fig. 11. Strain rate Davidenkov plot as proposed for DB and BD transitions at low and high strain rates. The general influence of temperature is indicated by the arrow. (redrawn from O'Connell et al. (2002) [7] with kind permission of John Wiley and Sons).

a rheological measurement such as the determination of the total entanglement density in a melt, $\zeta > 2$ is required. For a typical solid state mechanical measurement which occurs at longer time scales and higher stress fields a typical value of ζ greater than 7–10 is required [47].

Deblieck et al. independently obtained $\zeta \approx 7$ from an advanced rubber elastic analysis of the elastically active density contribution to strain hardening in low crystalline plastomers [49] using Klüppel's formulation of Heinrich's rubber elastic model [50–52] assuming Haward and Thackray's model [53]. The same result follows from the analysis of the strain hardening modulus of PE's using the Edwards Vilgis model [54] under the same assumptions [49]. In that model, the stress built up in a rubber network allows for a slipping contribution to the network response. It is found that the number of slipping links is typically an order of magnitude larger than the contribution of the fixed network [48,49,55].

The physical nature of the molecular entanglement network can be studied directly by means of solid state NMR which allows to separate the contribution from the time dependent junctions (temporary chain entanglements) and fixed crosslinks (trapped chain entanglements and permanent crosslinks either from chemical or physical origin) to the network relaxation [56–58].

It is the opinion of the authors that a deeper physical understanding of the time, temperature behaviour of polymers will require solid state NMR experiments under strain.

6.2. From effective entanglements to the strain hardening modulus

In 1968, Haward and Thackray [53] made the first attempt to interpret stress–strain data within a thermodynamic framework whereby the enthalpic yield processes are separated from the entropic network response of strain hardening. Within this simplified but powerful approach the strain hardening part is considered to be a purely entropic response of the entanglement network. The strain hardening modulus is considered to be proportional with the node density of the entanglement network. Haward carefully compared rheological rubber plateau modulus G_0^N, as obtained from the height of the rubber plateau in the polymer melt, with the strain hardening modulus G_p obtained assuming that the strain hardening response of a solid is purely rubber elastic, be it Gaussian or non-Gaussian. This approach proved to lead to the right order of magnitude and sometimes even equality of G_p to G_0^N [59,60]. Higher values were attributed to an increase in the effective entanglement density due to higher molecular mass and lower polydispersity [63]. Although this entropic increase is expected to have a major influence, the possibility of an enthalpic contribution from crystallinity cannot be excluded as it will be discussed in the next section.

Because the resistance of a stretched fibril within a craze to failure according to Equation (6) is proportional with the square of the number of loaded chains or the effective entanglement density, and because the strain hardening modulus, reflects the effective node density of the polymer molecular network, the critical strain energy release rate may be rewritten as in Equation (8):

$$G_{1c} \propto \left(G_p\left(\dot{\varepsilon}, M, T\right)\right)^2 \tag{8}$$

with

$$G_p = \upsilon_e RT = A\Sigma_e RT \tag{9}$$

where G_p is the strain hardening modulus in the solid state and it is assumed that Σ_e. is proportional to ν_e as it was shown by Van Melick et al. Equation (9) is the basic assumption for the hypothesis that G_p would be a valid measure to predict the resistance to SCG. Because relation (8) predicts proportionality with G_p^2 the logarithm of the toughness measure under consideration is mostly used to linearly correlate to G_p.

There is, however, a major problem with the measurement of G_p, when this is derived from a tensile test performed at room temperature as it will become apparent in the next section.

6.3. What does the strain hardening modulus represent?

Analysis of the strain hardening response may be performed using rubber elastic models based both on Gaussian and Langevin molecular statistics following the Haward–Thackray [53] model. This approach leads to insertion of an extra interpolated yield stress term σ_y^* to describe the enthalpic part:

$$\sigma_{true} = \sigma_y^* + \lambda\frac{\partial F}{\partial \lambda} = \sigma_y^* + G_p\left(\lambda^2 - \frac{1}{\lambda}\right)\Psi(\lambda, n) \tag{10}$$

where G_p was defined before in Equation (9) and Ψ takes into account the non-Gaussian chain statistics at large strains. For Gaussian statistics $\Psi = 1$ and Equation (10) reduces to the well-known Neo-Hookean, or Gaussian model. It is perhaps redundant to emphasise at this stage that Equation (10) inherently assumes that entropic and enthalpic contributions are separated mechanisms. In other words, that they are factorisable in free energy contribution, where the yield stress is entirely attributed to the deformation enthalpy of crystals at low deformation and the network part is purely entropic and entirely attributed to the ongoing orientation of molecular chain segments. For rubbery materials or semi-crystalline materials with low crystallinity and/or at elevated temperatures, the value of σ_y^* is generally small compared with the stresses measured at high deformations, typically a few MPa.

Within the Haward–Thackray approach, when a polymer is loaded beyond yield stress, the enthalpic contribution of crystals and/or chain friction is considered to be overcome. From literature on measuring and analysing the network response of a polymer in strain hardening it is found that for low density polyolefines [59,61,62] featuring a low crystallinity, the value of G_p as determined from a tensile experiment at room temperature, is usually of comparable order of magnitude as the entanglement density obtained from melt rheology [62], the so-called rubber plateau modulus. This indicates that in these cases the Haward–Thackray assumption is a useful and valid approximation.

For polymers with a high crystallinity, intractable crystals and also for glassy amorphous polymers with strong secondary interactions [63,64], however, the strain hardening response greatly exceeds the rheological entanglement density. Although Haward [59] attributed this to an increase in the number of effective entanglements due to an increase in molecular mass, the strain hardening modulus should still be comparable to the melt plateau modulus G_0^N beyond the yield stress and decrease with decreasing temperature. Instead it is observed that G_p is typically twice to an order of magnitude larger than G_0^N and increases with decreasing temperature. In 2005, Kramer [65] drew the attention of the materials science community to this discrepancy following the work of Van Melick et al. [64]. Recently, from theoretical calculations, Robbins et al. [66] found that in fact the strain hardening modulus scales linearly with the yield stress for a number of glassy polymers. This was later investigated experimentally by Govaert et al. [67] who found that although there seems to be a definite correlation, the scaling relation proposed by Robbins' calculations is not confirmed. The dependency of the strain hardening modulus on the yield behaviour is of major importance because it implies that the strain hardening of a polymer contains enthalpic contributions

that make the strain hardening scale with the amount of secondary interactions. This invalidates the Haward and Thackray model, at least at temperatures far below T_g or for semi-crystalline polymers: far below the α-transition.

The Bauschinger effect was introduced formally as an internal stress into the Hill anisotropic yield criterion to explain the difference between the tensile and compressive yield stresses parallel to the principal orientation direction in oriented polymers [69]. In a later paper, it was explicitly identified as a frozen in network stress to explain the yield and thermoelastic behaviour of oriented polymethylmethacrylate [70]. Govaert et al. [68] used the Bauschinger effect to separate the enthalpic contribution from the true network response for the strain hardening modulus. They suggested that in oriented polymers it can be explained by the introduction of a viscous contribution to the strain hardening in terms of a deformation dependence of the flow stress.

As expected, the enthalpic contribution to strain hardening also occurs in semi-crystalline polymers. This is demonstrated by comparing the strain hardening moduli at different temperatures as reported for PP [72]. If the strain hardening is solely caused by the entropy of an effectively entangled network this decrease should not occur, rather the reverse should happen. Thereby the conclusion that at lower temperatures the strain hardening modulus must contain enthalpic contributions is supported.

It is important to realise that the enthalpic effect will lead to an overestimation of the strain hardening values but that on the other hand these enthalpic contributions will be time dependent, unlike the entropic part. So, for longer load times the enthalpic contribution will tend to vanish. The strain hardening modulus will tend towards its entropic value when the strain rate is decreased. Ultimately, since creep failure resistance and long loading times are envisaged, the strain hardening measurement should reflect the entropic network contribution and the enthalpic part should be avoided as much as possible. This actually means that it is good practice to reduce the enthalpic part by decreasing the yield stress as much as possible.

According to the work of G'Sell et al. [72] who investigated the constitutive behaviour of PP at different temperatures up to 150 °C, the strain hardening of PP becomes relatively independent of strain rate at a temperature of about 110 °C, indicating that enthalpic effects have largely been overcome.

This is why it is suggested [9] to perform the strain hardening measurement at the α-transition temperature of PE, to eliminate the enthalpic contributions as much as possible i.e. it should take only a minor stress to overcome the crystal coherence. The mechanism of oncoming mobility of polymer chains with respect to crystals at the α-transition temperature was shown by direct evidence using solid state NMR and reported by Hu and Schmidt-Rohr et al. [71]

Now that it has been established that there are strong conceptual arguments in favour of relating the strain hardening response of a material to its resistance to SCG failure it is useful to give some attention to evidence for this relation.

7. Relation of SCG resistance to strain hardening for PE

As mentioned before, polyolefines can be used in applications with long service lifetimes e.g. utility pipes. As a result, high demands with respect to material properties (e.g. RCP, SCG) are set in standards to which the material has to comply. In general these standards require laborious and lengthy measurements to assess the long term SCG resistance usually referred to as Environmental Stress Cracking Resistance (ESCR) of the raw material.

Generally, the long term SCG resistance is assessed via tests that are accelerated by preliminary notching, increasing stress during measurement, measurement temperature and finally by adapting the environment by the addition of soap [74]. However, even then the assessment may take up to months. A great number of ESCR evaluation methods exist such as Notched Pipe Test (NPT), Pennsylvania Edge Notch Test (PENT) and Full Notched Creep Test (FNCT).

It would be advantageous to be able to rank materials in shorter testing times using lab scale amounts of material. The relation between SCG and the molecular network density, and by extension the strain hardening modulus as described above, is a valid basis to formulate such test methods.

Material intrinsic evaluation methods aimed at predicting the resistance to slow crack have been formulated by Rose and Cawood et al. [4,5] and O'Connell et al. [6,7]. The slow crack propagation step was approached via the creep rate deceleration of drawn PE samples. In their approach, they simulated the fibrillar structure within a craze by a tensile bar drawn to its natural draw ratio (NDR). A uniform relation between the creep rate deceleration of the drawn material and the growth was found. Cawood et al. [4] also showed that there is a direct relationship between the creep rate deceleration in a drawn sample and an ESCR measurement. Because creep rate deceleration is directly related with strain hardening via the unique true stress – true strain – true strain rate hypersurface of a material, the observations of O'Connell et al. and Cawood et al. are in fact equivalent to the approach followed in the present article.

Lagaròn et al. [8] showed by means of Raman Spectroscopy under tensile load that the inter-lamellar tie molecules in high SCG resistant PE samples bear less load than in low SCG resistant samples. This is a clear and independent indication of the importance of the network of tie molecules governing the creep resistance of fibrils.

Kurelec et al. [9] and later McCarthy et al. [12] built on those insights to propose the amount of strain hardening observed in a tensile test as a simple and robust measure of fibril deformation resistance. The strain hardening modulus $<G_p>$ as defined by Kurelec et al. turns out to correlate well with the resistance to SCG for a series of blow moulding PE grades.

Laurent [10] observed a sound correlation of resistance to SCG with the NDR, which is directly related to the amount of strain hardening via the Considère construction.

Cazenave, Séguéla et al. [11] also propose the NDR as a measure of the network response in an elegant and useful review. Their observations are substantiated by measuring creep compliance, NDR and morphological characterisation of crystallisation segregated samples by means of small angle X-Ray scattering of a series of high to medium density PE's of varying origin. This allowed them to investigate in more detail the influence of molecular structure on the tie molecule network density. Their work convincingly confirms the importance of the molecular network density for resistance to SCG.

Krishnashwami et al. and Sukadia et al. suggest that the natural draw-ratio is thought to be a consequence of inter-lamellar tie-molecule concentration and is therefore considered to be a reasonable indicator of the long-term fracture behaviour and durability of PE products [80,81].

Various experimental results support these statements. Historically, the first reference of the importance of the molecular network response for SCG in PE a series of PE's was reported by Rose et al. [5] in terms of correlation of the creep rate deceleration factor and the ESCR obtained from a bottle stress crack resistance test as shown in Fig. 12.

In 2005, Kurelec et al. [9] published the results of the correlation between the strain hardening modulus and the ESCR based on HDPE grades for blow moulding applications as shown in Fig. 13. In

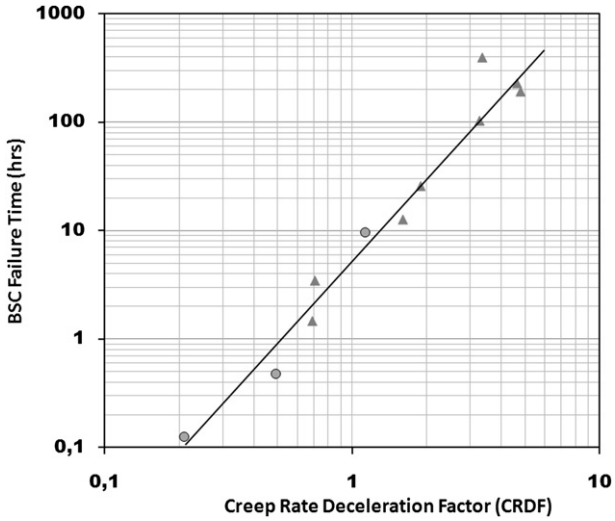

Fig. 12. Environmental bottle stress crack resistance (BSC) of PE homopolymers and copolymers as a function of creep rate deceleration factor (CRDF) (data taken and replotted from Rose et al. (1994) [5] with permission of Wiley & Sons).

2008, McCarthy et al. [12] extended this correlation for HDPE pipe grades.

Seguela [11,79] demonstrated the validity of the network density concept by correlation between ESCR data and the NDR, which is mechanically equivalent with the strain hardening modulus, as shown in Fig. 14 Sukhadia et al. [81] also use the NDR on a broader range of ESCR lifetimes as shown in Fig. 15.

Finally, a broader range of HDPE's was evaluated by van Beek et al. [73] for both FNCT and strain hardening, which resulted in the correlation shown in Fig. 16.

All the above experimental results support that the intrinsic strain hardening is a good measure for the intrinsic material resistance to SCG. These correlations make it plausible to state that the strain hardening response is determined by the same molecular differences that govern SCG resistance as measured by an ESCR test.

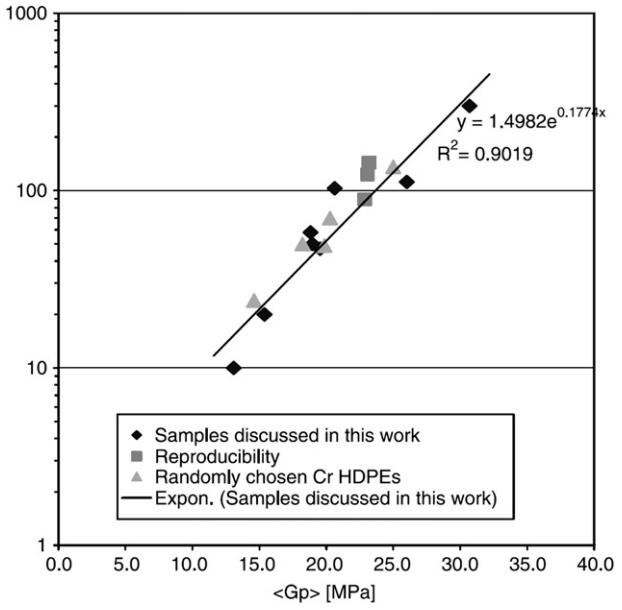

Fig. 13. ESCR as a function of the strain-hardening modulus $<G_p>$ for a series of HDPE materials (reproduced from Kurelec et al. (2005) [9] with kind permission of Elsevier).

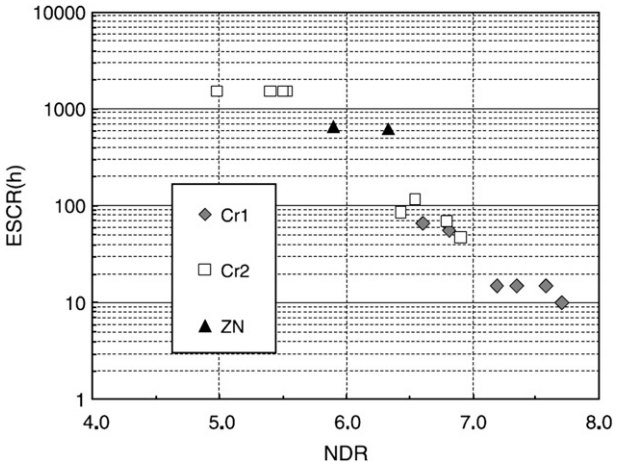

Fig. 14. ESCR versus NDR for a series of PE's with varying polydispersity reproduced from Cazenave et al. (2006) [11] with kind permission of Elsevier.

An alternative approach to analyse and rank the materials intrinsic resistance to SCG is possible. Starting from the phenomenology of fracture initiation under creep load, SCG may also be tackled as the static load limit of a fatigue failure. A fracture mechanics based analysis of such fatigue failure experiments has proven to be successful in ranking the SCG resistance performance of polyolefines [83,84].

7.1. Lessons learnt: how to increase the resistance to brittle failure?

Following the framework presented in this paper the strategies to avoid brittle failure require the shear yield stress to be lower than the craze stress. When this cannot be achieved the craze stress should at least be increased as much as possible. The main strategy to increase the craze stress consists of increasing the effective entanglement density as this will prevent craze propagation as well as craze failure. As it is generally known this can be achieved by increasing the molecular mass [9,49,59,61–63], by cross-linking and increasing the strain rate of the load, thus using the dynamic response of temporary entanglements [55]. It is less commonly known that adding short chain branches by copolymerisation of ethene [3,61] or propene [75] with 1-butene, 1-hexene or 1-octene

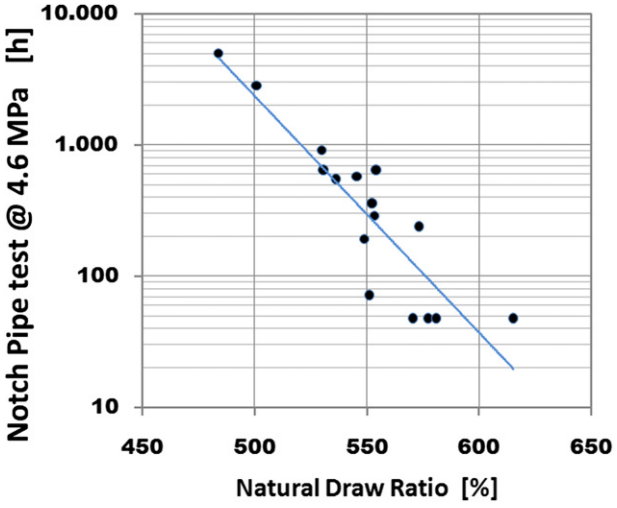

Fig. 15. ESCR response from Notched Pipe Test for a series of HDPE's versus the NDR (data taken from Sukhadia et al. (2010) [85] and replotted on a logarithmic scale).

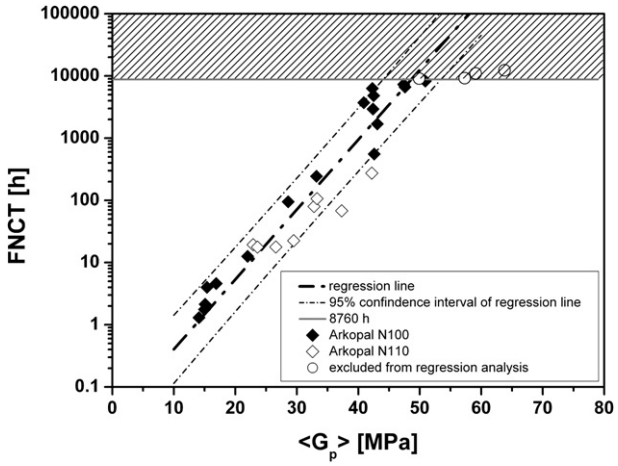

Fig. 16. Strain Hardening modulus $<G_p>$ versus FNCT for a very wide range of FNCT failure times taken from Van Beek et al. (2010) [73]. Failure times in FNCT above 1 year (grey area) are discarded from the statistical regression analysis because of the ongoing depletion of the stabiliser pack, and the possibility of premature failure due to molecular degradation.

and reducing the polydispersity [3,49] also increases the effective entanglement density [82].

As far as processing is concerned, toughening requires fast cooling so as to increase the number of tie molecules.

Furthermore, fast cooling, high molecular masses and short chain branching will also reduce the shear yield stress, because of the reduced crystallinity and increased crystalline disorder. The concepts of branching and increasing molecular mass are recognised and currently used in the development in bimodal HDPE pipe grades [77].

Besides strategies that influence the physical deformation mechanism by changing the molecular network it is also possible to influence the intrinsic stress situation.

A common strategy to influence the local stress state is rubber or void toughening. This strategy is used to toughen PP below T_g. The underlying concept is that a finely dispersed rubber phase cavitates under the local plane strain load [34]. Upon cavitation the load situation in the intermediate matrix ligaments reduces to plane stress. This favours shear deformation over crazing.

In this case, the network density of the matrix material will determine the critical thickness of the ligaments for shear to occur. Magalhães and Borggreve showed by means of an elegant SAXS experiment on a series of polystyrene rubber blends, whereby scattering from cavitation and crazing were discerned, that cavitation precedes the intrinsic deformation mechanism of the polystyrene matrix. Therefore, by increasing the rubber content and hence reducing the matrix ligament thickness between the rubber particles, the failure mechanism shifts from crazing to shearing [76]

Finally, strategies aimed at adding plasticisers so as to reduce the shear yield stress do not work, because adding effective plasticising agents also reduces the van der Waals surface energy and concomitantly the craze stress.

7.2. What remains to be done? an outlook

From the above discussion it becomes clear that the nature of the molecular network is ultimately important for understanding the failure behaviour of polymers either semi-crystalline or amorphous. It was also demonstrated that the time dependence, the dynamics of that molecular network is underlying a physical understanding of mechanical properties based on the knowledge of the molecular structure. We surmise that rheological investigations of carefully chosen model systems aimed at determining the scaling relations between molecular topology as studied with, for example, neutron scattering techniques and the molecular network are needed. Examples of such work have already been published [46,82,86,87]. A direct physical probe into the molecular network is provided by the aforementioned low field solid state NMR work [56–58,88]. Understanding the influence of short chain and long chain branching, the distribution and length of branches over the molecules in the material, the shape of the molecular mass distribution will also require state of the art molecular characterisation methods [90–92]. Such thorough characterisation allows establishing the component contribution to the long term failure resistance[93,94].

Finally, studies aimed at an advanced mechanical characterisation of the solid state strain hardening response, allowing to separate clearly the entropic from the enthalpic contributions as being undertaken by Govaert [68] et al. and Ward et al. [89] using the Fotheringham and Cherry stress dip test will be crucial to build proper structure property relations.

8. Conclusions

The main conclusions may be summarised as:

1) Existing models for craze initiation, craze propagation and craze–crack transition explain why the polymer network coherence determines the resistance to SCG.
2) The competition between crazing and shearing deformation mechanisms explains why at higher temperatures, longer times or lower strain rates, there exists a second Ductile–Brittle (DB) transition driven by chain disentanglement.
3) SCG in semi-crystalline polymers can be avoided by increasing the effective entanglement density, which is reflected by the strain hardening modulus measured above the temperature where collective segmental motion sets in (i.e. for PE, higher than the α-transition).
4) The correlation between the strain hardening modulus and the SCG resistance that follows from our considerations is valid for a very wide range of high density PE's.
5) Although the present framework already highlights the importance of the molecular network a further advanced characterisation of the molecular structure, rheology, chain dynamics and strain hardening response is still needed to establish comprehensive understanding of the intrinsic deformation and failure behaviour of polyolefines.

Acknowledgements

Dr Victor Litvinov is acknowledged for discussion on the physical nature of the molecular entanglement network.

References

[1] Plummer CJG, Goldberg A, Ghanem A. Polymer 2001;42:9551–64.
[2] Riemslag T. Crack Growth in PE. PhD Thesis: TU Delft; 1997, ISBN: 90-407-1453-3.
[3] Thomas C, Ferreiro V, Coulon R, Seguela R. Polymer 2007;48:6041–8.
[4] Cawood MJ, Channell AD, Capaccio G. Polym Commun 1993;32:423–5.
[5] Rose LJ, Channell CJ, Capaccio GJ. Appl Polym Sci 1994;54:2119–24.
[6] O'Connell PA, Bonner MJ, Duckett RA, Ward IM. Polymer 1995;36:2355–62.
[7] O'Connell PA, Duckett RA, Ward IM. Polym Eng Sci 2002;42:1493–508.
[8] Lagarón JM, Capaccio G, Rose L, Kip BJ. J Appl Polym Sci 2000;77:283–96.
[9] Kurelec L, Teeuwen M, Schoffeleers H, Deblieck R. Polymer 2005;46:6369–79.
[10] Laurent E, Proceedings of Plastics Pipes XI; 2001.
[11] Cazenave J, Seguela R, Sixou B, Germain Y. Polymer 2006;47:3904–14.
[12] McCarthy M, Deblieck R, Mindermann P, Kloth R, Kurelec L, Martens H. In: Plastic Pipes XIV Conference, Budapest, Hungaria; September 22–24 2008.

[13] Grellmann W, Seidler S. Deformation and fracture behaviour of polymers. In: Springer series engineering materials. Berlin. Heidelberg, New York: Springer-Verlag, ISBN 3-540-41247-6; 2001.
[14] Ward IM. Mechanical properties of solid polymers. Chichester: John Wiley and Sons; 1983.
[15] Kambour RP. J Polym Sci Macromol Rev 2008;7:1.
[16] Donald AM, Kramer EJ. Philos Mag 1981;43:857.
[17] Donald AM. J Mater Sci 1985;20:2630–8.
[18] Donald AM, Kramer EJ. J Mater Sci 1982;17:1871–9.
[19] Berger L, Kramer E. Macromolecules 1987;20:1980–5.
[20] Kramer E. Adv Polym Sci; 1983:52–3.
[21] van Melick HGH, Bressers OFJT, den Toonder JMJ, Govaert LE, Meijer HEH. Polymer 2003;44:2481–91.
[22] Argon AS. Philos Mag 1973;28:839.
[23] Plummer CJG, Cudré-Mauroux N, Kausch H-H. Polym Eng Sci 1994;34(4):318–29.
[24] Kramer E, Berger L. Adv Polym Sci; 1990:91–2.
[25] Brown HR. Macromolecules 1991;24:2752–6.
[26] Argon AS. J Macromol Sci Phys 1973;B8(3–4):573–96.
[27] Hui C, Ruina A, Creton C, Kramer E. Macromolecules 1992;25:3948–55.
[28] Kausch H-H. Polymer fracture. 2nd ed. Berlin: Springer Verlag; 1987.
[29] Odell JA, Keller A. J Polym Sci Polym Phys Ed 1986;24:1889–916.
[30] Kambour RP. Polym Commun 1983;24:292.
[31] Wu S. Polym Int 1992;29:229–47.
[32] Bucknall C, Smith R. Polymer 1965;6:437–46.
[33] Michler GH. J Macromol Sci Phys 1999;B38(5&6):787–802.
[34] Borggreve RJM, Gaymans RJ, Schuijer J. Polymer 1989;30:71–7.
[35] Borggreve RJM, Gaymans RJ, Eichenwald HM. Polymer 1989;30:78–83.
[36] Wu SJ. Appl Polym Sci 1988;35:549–61.
[37] van der Wal A, Mulder JJ, Oderkerk J, Gaymans RJ. Polymer 1998;39:6781–7.
[38] van der Wal A, Nijhof R, Gaymans RJ. Polymer 1999;40:6031–44.
[39] van der Wal A, Gaymans RJ. Polymer 1999;40:6045–55.
[40] van der Wal A, Verheul AJJ, Gaymans RJ. Polymer 1999;40:6057–65.
[41] van der Wal A, Gaymans RJ. Polymer 1999;40:6067–75.
[42] Donald AM. Personal communication; 1995.
[43] Wu S. J Polym Sci B Polym Phys Ed 1989;27:723–41.
[44] Wu S. Polym Eng Sci 1990;30:753–61.
[45] Wu S. Polym Eng Sci 1992;32:823–30.
[46] Fetters L, Lohse D, Richter D, Witten T, Zirkel A. Macromolecules 1994;27(17): 4639–47.
[47] Mikos A, Peppas N. J Chem Phys 1988;88(2):1337–42.
[48] Deblieck R. Internal DSM report 1999-15164RC; 1999.
[49] Deblieck R, Lemstra P. Conference preprints 11th Int. Conf. On deformation yield and fracture of polymers 10–13 April 2000 Churchill College Cambridge, UK. London: IOM Communications Ltd, ISBN 1-86125-120-3; 2000. p. 531–534.
[50] Klüppel M. J Appl Polym Sci 1993;48:1137–50.
[51] Klüppel M, Heinrich G. Macromolecules 1994;(27):3596–603.
[52] Matzen D, Straube E. Colloid Polym Sci 1992;270:1–8.
[53] Haward RN, Thackray G. Proc Roy Soc Lond 1968;A302:453–72.
[54] Edwards SF, Vilgis Th. Polymer 1986;27:483–92.
[55] Brereton MG, Klein PG. Polymer 1988;29:970–1974.
[56] Litvinov VM, Barendswaard W, van Duin M. Rubber Chem Technol 1998;71: 105–18.
[57] Litvinov VM, Steeman PAM. Macromolecules 1999;32:8476–90.
[58] Litvinov VM. Macromolecules 2006;39:8727–41.
[59] Haward RN. Macromolecules 1993;26:5860–9.
[60] Mills PJ, Hay JN, Haward RN. J Mater Sci 1985;20:501–7.
[61] Bensason S, Stepanov EV, Chum S, Hiltner A, Baer E. Macromolecules 1997;30: 2436–44.
[62] Haward RN. Polymer 1999;40:5821–32.
[63] Haward RN. J Polym Sci Part B Polym Phys 2007;45:1090–9.
[64] van Melick HGH, Govaert LE, Meijer HEH. Polymer 2003;44:2493–502.
[65] Kramer EJ. J Polym Sci Part B Polym Phys 2005;43:3369–71.
[66] Robbins M, Hoy RS. J Polym Sci Part B Polym Phys 2009;47:1406–11.
[67] Govaert LE, Engels TAP, Wendlandt M, Tervoort TA, Suter UW. J Polym Sci Part B Polym Phys 2008;46:2475–81.
[68] Senden DJA, van Dommelen JAW, Govaert LE. J Polym Sci Part B Polym Phys 2010;48:1483–94.
[69] Brown N, Duckett RA, Ward IM. Philos Mag 1968;18:483–502.
[70] Botto PA, Duckett RA, Ward IM. Polymer 1987;28:257–62.
[71] Hu W-G, Schmidt-Rohr K. Acta Polym 1999;50:271–85.
[72] Duffo P, Monasse B, Haudin JM, G'Sell C, Dahoun A. J Mater Sci 1995;30:701–11.
[73] van Beek DJM, Deblieck R, McCarthy M, Kloth R, Kurelec L. Proceedings of Plastic Pipes XV, Vancouver, Canada, 2010.
[74] Hessel J, Hessel J. Qualitätssicherung für grabenlos verlegbare Rohre aus Polyethylen in Sonderdruk aus' 3R International', 40, Jahrgang, Heft 6, 2001, seiten 178–184.
[75] Poon B, Rogunova M, Hiltner A, Baer E, Chum SP, Galeski A, et al. Macromolecules 1999;38:1232–43.
[76] Magalhães AML, Borggreve RJM. Macromolecules 1995;28:5841–51.
[77] Brömstrup H. PE 100 p.pe systems. 2nd ed. Vulkan Verlag GmBh; 2004.
[78] Kausch HH, Michler GH. Adv Polym Sci 2005;187:1–33.
[79] Séguéla R. Macromol Mater Eng 2007;292:235–44.
[80] Krishnaswamy RK, Yang Q, Fernandez-Ballester L, Kornfield JA. Macromolecules 2008;41:1693–704.
[81] Sukhadia AM, Lamborn MJ, Deslauriers PJ, Garcia RA. Plastic pipes XV. Vancouver, Canada; September 2010.
[82] García-Franco CA, Harrington BA, Lohse DJ. Macromolecules 2006;39:2710–7.
[83] Frank A, Freimann W, Pinter G, Lang RW. Eng Fract Mech 2009;76:2780–7.
[84] Zhou Z, Hiltner A, Baer E. J Mater Sci 2011;46:174–82.
[85] Sukhadia AM, Lamborn MJ, Deslauriers PJ, Garcia RA, Domínguez C. In: Plastic Pipes XV Conference, Vancouver, Canada; September 20–22 2010.
[86] Abdel-Goad M, Pyckhout-Hintzen W, Kahle S, Allgaier J, Richter D, Fetters LJ. Macromolecules 2004;37:8135–44.
[87] Chen X, Stadler FJ, Münstedt H, Larson RG. J Rheol 2010;2(54):393–406.
[88] Cohen-Addad JP, Guillermo A. Macromolecules 2003;36:1609–15.
[89] Bonner M, Montes de Oca H, Brown M, Ward IM. Polymer 2010;51:1432–6.
[90] Macko T, Brüll R, Zhu Y, Wang Y. J Sep Sci 2010;33:3446–54.
[91] Chitta R, Macko T, Brüll R, van Doremaele G, Heinz LC. Separation of ethylene-propylene copolymers and ethylene-propylene-diene terpolymers using high temperature interactive liquid chromatography, J Polym Sci Part A Polym Chem 2011, accepted.
[92] Ginzburg A, Macko T, Dolle V, Brüll R. Eur Polym J 2011;47:319–29.
[93] Soares J, Abbott RF, Kim JD. J Polym Sci Part B Polym Phys 2000;38:1267–75.
[94] Stephenne V, Daoust D, Debras G, Dupire M, Legras R, Michel J. J Appl Polym Sci 2001;82:916–28.

Rudy Deblieck graduated from Brussels Free University (VUB) in theoretical physical chemistry in 1979 and got his PhD at University of Antwerp in Solid State Physics focussing on the study of soft mode phase transitions by means of Transmission Electron Microscopy and Wide Angle Xray Diffraction in 1986. He is currently employed as senior scientist in the polymer morphology group at DSM Resolve in the Netherlands and has been working for DSM since 1986 as group leader in Microscopy and Mechanical Properties. His main interest is in the structure morphology and structure property relations of polymers with a focus on polyolefines. In this respect he is currently acting as a full time dedicated consultant to the R&D work at SABIC T&I.

D.J.M. (Linda) Havermans – van Beek graduated at the Eindhoven University of Technology in Biomedical Engineering in 2003. In 2007, she obtained her PhD in Organic Chemistry in the same university under the supervision of Prof E. W. Meijer and Prof R.P. Sijbesma. The title of her PhD work is Reversible Networks in Supramolecular Polymers. She joined the Technology and Innovation department of SABIC in The Netherlands in 2008 as Materials Development Engineer. Presently, her main activities concern the developments within bimodal HDPE for utility pipe applications. She is particularly interested in structure–property relations.

Klaas Remerie graduated at Groningen University in Physical-Organic Chemistry and obtained his PhD in 1984 at the same university on kinetic and molecular dynamics studies of solvation effects on hydrolysis reactions in mixed water/organic solvents. After a few years at Ciba as a Research Coordinator Dispersed Pigments he joined DSM in 1988 as a Product Development Specialist Polypropylenes. After various management roles within DSM Research as well as DSM's Polypropylene Business Unit, he joined SABIC R&D again in 2002 when DSM Petrochemicals was integrated into the SABIC organization.Presently he is a senior scientist within the material development group of SABIC Europe R&D. In this role he is specifically assigned to longer term development activities with a focus on Polypropylenes.He also represents SABIC in the Program Committee Polyolefins of the Dutch Polymer Institute, and is involved in several co-operations between SABIC Europe R&D and various universities and other scientific institutes.

Professor **I M Ward**, received a D.Phil from Oxford University in 1954 for ESR studies of inorganic complexes and irradiated materials. From 1954 to 66 he undertook research at ICI Fibres Division, becoming Head of Basic Physics and an ICI Research Associate. After four years as Senior Lecturer in the Physics of Materials at Bristol University, he was appointed to a Chair of Physics at Leeds University in 1970 where he founded the Polymer Group and was Departmental Chair from 1974 to 1977 and 1987 to 1989. Subsequently in 1989, Professor Ward became first Director of the IRC in Polymer Science and Technology (now the Polymer IRC). He is presently Research Professor Emeritus. He was elected to the Royal Society in 1983 and has been awarded several medals by the Institute of Materials (Griffith, Swinburne, Netlon) and the Institute of Physics (C.V. Boys, Glazebrook).